

Gravitational lensing and time delay for the charged black holes with scalar hair

Ruanjing Zhang and Jiliang Jing^{*}

Department of Physics, Key Laboratory of Low Dimensional Quantum Structures and Quantum Control, Ministry of Education, Hunan Normal University, Changsha, Hunan 410081, People's Republic of China

ABSTRACT: The gravitational lensing and time delay for charged black holes with scalar hair in Einstein-Maxwell-Dilaton theory are studied. We find, with the increase of scalar hair, that the radius of the photon sphere, minimum impact parameter, angular image position and relative magnitude increase, while the deflection angle and angular image separation decrease. We also show, for the primary relativistic image which is formed by the light does not loop around the lens and situated on the same side of the source, that the scalar hair increases the time delay. Our results can be reduced to those of the Schwarzschild black hole.

KEYWORDS: gravitational lensing; time delay; scalar hair; black hole.

^{*}Corresponding author. Email: jljing@hunnu.edu.cn

Contents

1. Introduction	1
2. Deflection angle for charged black holes with scalar hair	3
3. Observables in gravitational lensing	10
4. Time delay for charged black holes with scalar hair	13
5. Summary	15

1. Introduction

The presence of a massive body produces the deflection of light passing close to the object according to the theory of general relativity; the corresponding effects are called as gravitational lensing, and the object causing a detectable deflection acts as gravitational lens [1]. What's more, this deflection of light was first observed in 1919 by Dyson, Eddington, and Davidson [2]. After the pioneering strong gravitational lensing in Q0957+561 [3] was discovered in 1979, gravitational lensing developed into an important astrophysical tool to extract information about distant stars which are too dim to be observed, similar to a natural and large telescope. When an object with a photon sphere is situated between a source and an observer, in addition to primary and secondary images due to small deflections of the light rays, there are two infinite sets of images called relativistic images, produced by light passing close to the photon sphere, which undergoes a large deflection. It is shown that these relativistic images carry much valuable information about the central celestial objects and could provide the profound verification of alternative theories of gravity [4, 5, 6, 7, 8, 9, 10, 11, 12, 13, 14, 15, 16]. Therefore, gravitational lensing is

regarded as a powerful indicator of the physical nature of the central celestial object. So, we need a systematic approach to calculate the deflection angle and the feature of relativistic images. Darwin [17] calculated the deflection angle by using the strong deflection limit (consisting of a logarithmic approximation) for the Schwarzschild spacetime. And this method allows for calculating the position, magnification of the relativistic images. It was rediscovered several times [18], then extended to the Reissner-Nordström metric [19], and to any spherically symmetric objects with a photon sphere [20]. A lot of works [21] have been done basing on this method. Virbhadra [22, 23] studied the time delay for the Janis-Newman-Winicour naked singularities black hole and the Schwarzschild black hole by using numerical method, and he did not take either weak or strong field approximation. As a result, this method has very good accuracy, and we will study the time delay following it.

The standard “no-hair theorem” [24] states that a black hole is completely specified by the mass, charge, and angular momentum. However, during the recent years, much attention was devoted to gravity theories supplying by scalar field, and many examples of scalar hairy black holes [25, 26, 27, 28] have been obtained. There are several reasons for this. To begin with, as one kind of the fundamental and effective fields, scalar field is well motivated by standard-model particle physics. In addition, we analyze different field contents which can be treated as a means of checking the “no-hair theorem” and exploring the structure of black holes. Scalar field is often considered by physicists as one of the simplest types of “matter”. At last, the presence of the scalar field leads to different black hole spacetimes, which may engender some new phenomena. We hope these deviations could be detected in astrophysical observations. What’s more, the fundamental scalar field does exist in nature by discovering a scalar particle at the Large Hadron Collider at CERN [29, 30], which has been identified as the standard-model Higgs boson since 2012. Therefore, to study gravitational lensing and time delay for black holes with scalar hair has great significance.

This paper is arranged as follows: In Sec. 2, we study the physical properties of gravitational lensing around the charged black holes with scalar hair and probe the effects of the scalar hair on the event horizon, the radius of the photon sphere, the minimum impact

parameter, and the deflection angle. In Sec. 3, we suppose that the gravitational field of the supermassive black hole at the centre of our Galaxy can be described by this metric, and then obtain the numerical results for the main observables in gravitational lensing, such as the angular image position, angular image separation, and relative magnitude of relativistic images. In Sec. 4, we study the time delay for the primary relativistic image, which is formed by the light does not loop around the lens and situated on the same side of the source. Finally, we will include our conclusions in the last section.

2. Deflection angle for charged black holes with scalar hair

Supergravities have provided a variety of fundamental matter fields that we can study their interactions with gravity [31, 32, 33, 34, 35], one of them is dilatonic scalar [36]. If the dilaton ϕ couples to an n -form field strength $F_n = dA_{n-1}$ through $Z(\phi)$, the general class of Lagrangian is given by [37]

$$e^{-1}\mathcal{L} = R - \frac{1}{2}(\partial\phi)^2 - \frac{1}{2n!}Z(\phi)F_n^2, \quad (2.1)$$

where $e = \sqrt{-\det(g_{\mu\nu})}$. It is not hard to find that we can get the usual Reissner-Nordström black hole decoupled with the dilaton if $Z(\phi)$ in Eq. (2.1) has a stationary point. And the uniqueness theorem is broken if we can construct a further different black hole with the same mass and charge, but non-vanishing dilaton. Now, we suppose Z as

$$Z^{-1} = e^{a_1\phi} \cos^2 \omega + e^{a_2\phi} \sin^2 \omega, \quad (2.2)$$

with

$$a_1 a_2 = -\frac{2(n-1)(D-n-1)}{D-2}, \quad (2.3)$$

where a_1 and a_2 are the dilaton coupling constants, and ω is another coupling constant. The function Z becomes an exponential function of ϕ for $\omega = 0$ or $\omega = \frac{\pi}{2}$.

In this paper, we focus our attention on the Einstein-Maxwell-Dilaton theory in four dimensions, corresponding to $D = 4$ and $n = 2$, in which the dilaton ϕ coupling to the Maxwell field A is not the usual single exponential function, but one with a stationary

point. The condition for (a_1, a_2) in Eq. (2.3) becomes $a_1 a_2 = -1$, and then the Lagrangian can be rewritten as

$$e^{-1} \mathcal{L} = R - \frac{1}{2}(\partial\phi)^2 - \frac{1}{4}ZF^2, \quad (2.4)$$

where $F = dA$. The constants a_1, a_2 can be expressed as

$$a_1 = \sqrt{\frac{1-\mu}{1+\mu}}, \quad a_2 = -\sqrt{\frac{1+\mu}{1-\mu}}. \quad (2.5)$$

The dilaton coupling function Z is thus given by

$$Z^{-1} = e^{\sqrt{\frac{1-\mu}{1+\mu}}\phi} \cos^2 \omega + e^{-\sqrt{\frac{1+\mu}{1-\mu}}\phi} \sin^2 \omega. \quad (2.6)$$

Then, the Lagrangian (2.4) admits the charged black holes with scalar hair as [37]

$$ds^2 = -f(r)dt^2 + \frac{dr^2}{f(r)} + r^{1+\mu}(r+S)^{1-\mu}(d\theta^2 + \sin^2 \theta d\phi^2), \quad (2.7)$$

where

$$f(r) = \left(1 + \frac{S}{r}\right)^\mu \left[1 + \frac{Q^2 \cos^2 \omega}{2rS(1+\mu)} - \frac{Q^2 \sin^2 \omega}{2S(1-\mu)(r+S)}\right]. \quad (2.8)$$

The solution involves two integration constants, one is constant Q which parameterizes the electric charge, the other is S that associates with dilaton ϕ by

$$e^{\frac{\phi}{\sqrt{1-\mu^2}}} = 1 + \frac{S}{r}. \quad (2.9)$$

Since the black hole has scalar hair with varying ϕ , S parameterizes the scalar hair.

What important is that this solution will return to the Schwarzschild black hole when $S \rightarrow 0$ or $\omega = \frac{\pi}{2}$ with $\mu \rightarrow 1$. Hence, this limit can be used to test our results in the following study. After that, the ADM mass, electric charge, and Maxwell field A are given by [37]

$$M = \frac{Q^2 \sin^2 \omega}{4(1-\mu)S} - \frac{Q^2 \cos^2 \omega}{4(1+\mu)S} - \frac{1}{2}\mu S, \quad Q_e = \frac{1}{4}Q, \quad A = \frac{Q(r+S \cos^2 \omega)}{r(r+S)}. \quad (2.10)$$

It is useful for the calculation to follow the scaling symmetries in the forms

$$\frac{r}{2M} \rightarrow r, \quad \frac{S}{2M} \rightarrow S, \quad \frac{Q}{2M} \rightarrow Q, \quad \frac{t}{2M} \rightarrow t, \quad \frac{C(r)}{(2M)^2} \rightarrow C(r). \quad (2.11)$$

After taking the scaling symmetries, the solution (2.7) still takes the same form as above. Since it is meaningful to study the effects of scalar hair on the gravitational lensing, we can use μ, ω, S to show Q^2 as

$$Q^2 = \frac{2S(1-\mu)(1+\mu)(1+S\mu)}{(\mu-1)\cos^2\omega + (\mu+1)\sin^2\omega}. \quad (2.12)$$

Then, we have to take $\omega \in [\frac{\pi}{4}, \frac{\pi}{2}]$ with $\mu = 0$ or $\mu \in (-1, 1)$ with $\omega = \frac{\pi}{2}$ to ensure $Q^2 > 0$.

Now, let us study the physical properties of gravitational lensing by the charged black holes with scalar hair. We choose the equatorial plane ($\theta = \frac{\pi}{2}$) which means that both the observer and the source lie in the equatorial plane, and the whole trajectory of the photon is limited on the same plane. Then the metric (2.7) can be expressed as

$$ds^2 = -A(r)dt^2 + B(r)dr^2 + C(r)d\phi^2, \quad (2.13)$$

with

$$A(r) = f(r), \quad B(r) = \frac{1}{f(r)}, \quad C(r) = r^{1+\mu}(r+S)^{1-\mu}. \quad (2.14)$$

In the spherically symmetric case, the equation of the photon sphere reads

$$\frac{C'(r)}{C(r)} = \frac{A'(r)}{A(r)}, \quad (2.15)$$

where the prime represents the derivative with respect to r . For the charged black holes with scalar hair, the equation of the photon sphere takes the form

$$\begin{aligned} & 8Sr^3(\mu^2 - 1) + r^2[4S^2(2\mu + 3)(\mu^2 - 1) + 6Q^2(\mu - \cos 2\omega)] \\ & + 2Sr[2S^2(2\mu^3 + \mu^2 - 2\mu - 1) + Q^2(2\mu^2 + 3\mu - 2 - 3\cos 2\omega)] \\ & + 2S^2Q^2(1 + \cos 2\omega)(\mu^2 - 1) = 0. \end{aligned} \quad (2.16)$$

Obviously, this equation has three roots because it is a cubic equation of r . We take the root tends to 1.5 when $S \rightarrow 0$ as the radius of the photon sphere. In other words, we take the root which could return to the Schwarzschild black hole when $S \rightarrow 0$. We present the variation of the radius of the photon sphere r_{ps} and radius of the event horizon r_H with the scalar hair S for $\mu = 0$ (varying ω) and $\omega = \frac{\pi}{2}$ (varying μ) in Fig. 1. We can see that r_{ps} always bigger than r_H for given μ and ω , this is in accordance with our usual perception. This black hole can recover to the Schwarzschild black hole [20] ($r_H = 1$, $r_{ps} = 1.5$) in two cases, one is $S \rightarrow 0$ for arbitrary ω and μ , another is $\omega = \frac{\pi}{2}$ and $\mu \rightarrow 1$ for arbitrary scalar hair S . From Fig. 1, we can see that each line of r_H and r_{ps} intersects when $S \rightarrow 0$, and the black line in the right figure is basically a straight line, these are both performances of recovering to the results of the Schwarzschild case.

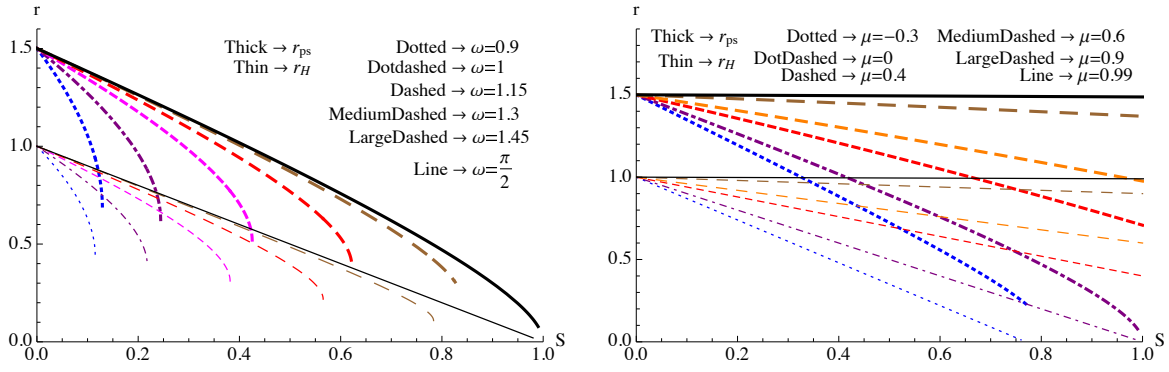


Figure 1: Radius of the photon sphere (thick line) and horizon (thin line) change with scalar hair S for $\mu = 0$ (left) and $\omega = \frac{\pi}{2}$ (right).

The exact deflection angle α for a photon coming from infinity, relates to the closest approach distance r_0 , can be expressed as [39]

$$\alpha(r_0) = I(r_0) - \pi, \quad (2.17)$$

with

$$I(r_0) = 2 \int_{r_0}^{\infty} \frac{\sqrt{B(r)} dr}{\sqrt{C(r)} \sqrt{\frac{C(r)A(r_0)}{C(r_0)A(r)} - 1}}. \quad (2.18)$$

The deflection angle is a monotonic decreasing function of r_0 . For a special value of r_0 , the deflection angle will become 2π , that is to say, the light ray will makes a complete loop

around the compact object before reaching the observer, which results in two infinite sets of relativistic images, one is on the same side, and the other is on the opposite side of the source. Furthermore, the deflection angle diverges when r_0 approaches to the radius of the photon sphere r_{ps} , which means that the photon is captured.

We are now in position to calculate the case of a photon passing close to the photon sphere, by using the evaluation method for the integral (2.18) proposed by Bozza [20]. Then, it is useful to define a new variable

$$z = 1 - \frac{r_0}{r}, \quad (2.19)$$

and we will obtain

$$I(r_0) = \int_0^1 R(z, r_0) f(z, r_0) dz, \quad (2.20)$$

with

$$R(z, r_0) = \frac{2r^2 \sqrt{A(r)B(r)C(r_0)}}{r_0 C(r)},$$

$$f(z, r_0) = \frac{1}{\sqrt{A(r_0) - \frac{A(r)C(r_0)}{C(r)}}}, \quad (2.21)$$

where $R(z, r_0)$ is the regular term, and $f(z, r_0)$ is the divergent term which diverges for $z \rightarrow 0$ —i.e., the photon approaches the photon sphere. So we can split the integral (2.20) as a sum of two parts

$$I_D(r_0) = \int_0^1 R(0, r_{ps}) f_0(z, r_0) dz, \quad (2.22)$$

$$I_R(r_0) = \int_0^1 [R(z, r_0) f(z, r_0) - R(0, r_{ps}) f_0(z, r_0)] dz, \quad (2.23)$$

where $I_D(r_0)$ and $I_R(r_0)$ denote the divergent and regular parts in the integral (2.20), respectively. To find the order of divergence of the integrand, we take a Taylor expansion of the argument of the square root in $f(z, r_0)$ to the second order in z ; then we get

$$f_0(z, r_0) = \frac{1}{\sqrt{p(r_0)z + q(r_0)z^2}}, \quad (2.24)$$

with

$$p(r_0) = \frac{r_0}{C(r_0)}(A(r_0)C'(r_0) - A'(r_0)C(r_0)), \quad (2.25)$$

$$q(r_0) = \frac{r_0}{2C^2(r_0)}(2r_0C(r_0)C'(r_0)A(r_0) - 2r_0C'^2(r_0)A(r_0) + r_0C(r_0)C''(r_0)A(r_0) - r_0C^2(r_0)A''(r_0)). \quad (2.26)$$

It is obviously that $p(r_0) = 0$ at $r_0 = r_{ps}$ from Eqs. (2.15) and (2.25). So we have $f_0(z, r_0) \sim \frac{1}{z}$ when r_0 is equal to the radius of the photon sphere r_{ps} , and then the term $I_D(r_0)$ diverges logarithmically. Therefore, the deflection angle can be expanded in the form

$$\alpha(\theta) = -\bar{a} \log\left(\frac{\theta D_{OL}}{u_{ps}} - 1\right) + \bar{b} + o(u - u_{ps}), \quad (2.27)$$

with

$$\begin{aligned} \bar{a} &= \frac{R(0, r_{ps})}{2\sqrt{q(r_{ps})}}, \\ \bar{b} &= -\pi + b_R + \bar{a} \log \frac{r_{ps}^2 [C'''(r_{ps})A(r_{ps}) - C(r_{ps})A''(r_{ps})]}{u_{ps} \sqrt{A^3(r_{ps})C(r_{ps})}}, \\ b_R &= I_R(r_{ps}), \\ u_{ps} &= \sqrt{\frac{C(r_{ps})}{A(r_{ps})}}, \end{aligned} \quad (2.28)$$

where the quantity D_{OL} is the distance between the observer and the gravitational lens; θ is the angular separation between the optical axis and the direction of image which satisfies $u = \theta D_{OL}$; u_{ps} is the impact parameter u evaluated at r_{ps} which is called the minimum impact parameter; \bar{a} and \bar{b} are strong deflection limit coefficients which depend only on the metric function evaluated at r_{ps} . Making use of Eqs. (2.27) and (2.28), we can study the properties of gravitational lensing by the charged black holes with scalar hair.

Now, we probe the properties of gravitational lensing by the charged black holes with scalar hair and mainly explore the effects of the scalar hair S on the deflection angle. We show, in Figs. 2-4, the variation of the coefficient \bar{a} , the minimum impact parameter u_{ps} , and the deflection angle $\alpha(\theta)$ with scalar hair S for the change of ω when $\mu = 0$, and for

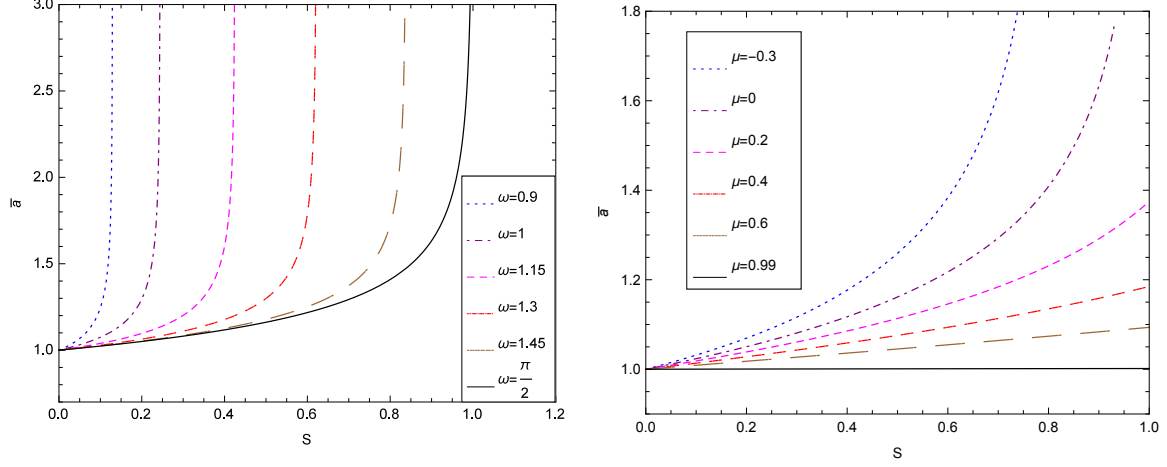


Figure 2: Variation of the coefficient \bar{a} with scalar hair S for $\mu = 0$ (left) and $\omega = \frac{\pi}{2}$ (right).

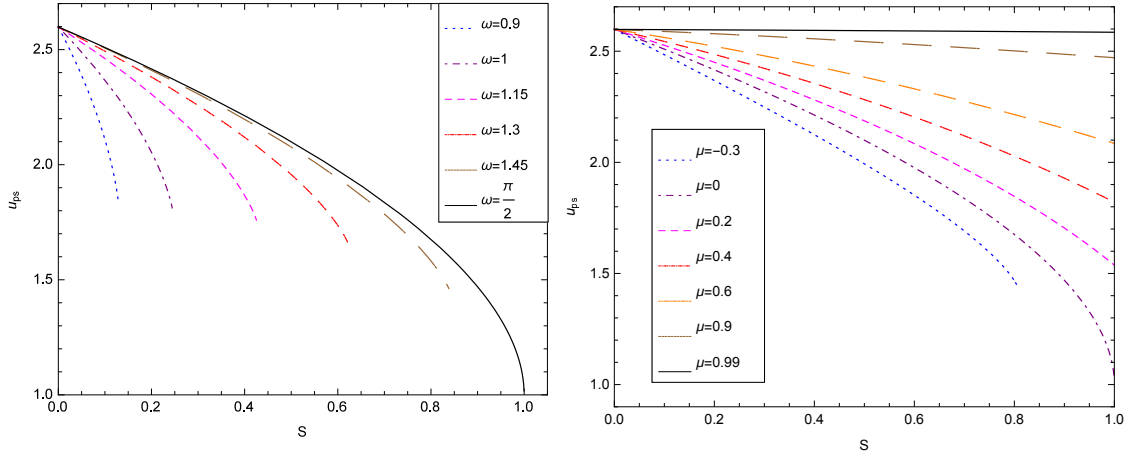


Figure 3: Variation of the minimum impact parameter u_{ps} with scalar hair S for $\mu = 0$ (left) and $\omega = \frac{\pi}{2}$ (right).

the change of μ when $\omega = \frac{\pi}{2}$, respectively. We can read from Fig. 2 that the coefficient \bar{a} always grows with the increase of scalar hair S for either $\mu = 0$ or $\omega = \frac{\pi}{2}$, but the growth rate decreases with the increase of μ or ω . Furthermore, we get that the minimum impact parameter u_{ps} decreases with the increase of scalar hair S for either $\mu = 0$ or $\omega = \frac{\pi}{2}$ in Fig. 3. We also plot the deflection angle $\alpha(\theta)$ evaluated at $u = u_{ps} + 0.003$ in Fig. 4. And then, we find that the deflection angle increases with the increase of scalar hair regardless of the varying μ and ω , which tells us that the scalar hair enhances the effects of the black hole on the light. It is also shown that the deflection angle has the similar

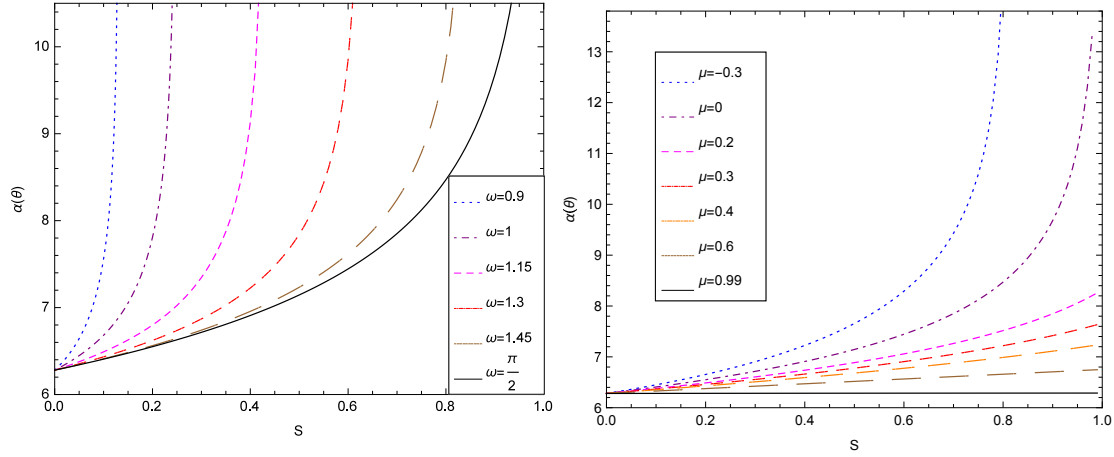


Figure 4: The deflection angle evaluated at $u = u_{ps} + 0.003$ as a function of scalar hair S for $\mu = 0$ (left) and $\omega = \frac{\pi}{2}$ (right).

properties with the coefficient \bar{a} ; this means that the deflection angle of the light ray is dominated by the logarithmic term in strong gravitational lensing. There is one thing that we can't ignore is every line of \bar{a} , u_{ps} , and $\alpha(\theta)$ intersects at $S \rightarrow 0$ for arbitrary μ and ω , which implies that they recover to the results of the standard Schwarzschild case [20]; i.e., $\bar{a} = 1$, $u_{ps} = 2.598$, and $\alpha(\theta) = 6.28$. We should also note that the black lines in each graph on the right side of Figs. 2-4 are almost straight lines, it means that our results recover to the results of the Schwarzschild case again for $\omega = \frac{\pi}{2}$ and $\mu \rightarrow 1$.

3. Observables in gravitational lensing

In this part, we calculate the observables in gravitational lensing by the charged black holes with scalar hair, including the angular image position θ_∞ , the angular image separation s , and the relative magnitude r_m . Let us start with the lens equation [20]

$$\beta = \theta - \frac{D_{LS}}{D_{OS}} \Delta\alpha_n, \quad (3.1)$$

where β is the angle between the direction of the source and the optical axis, called the angular source position. D_{LS} is the distance between the lens and the source; D_{OS} is the distance between the observer and the source, and they satisfy $D_{OS} = D_{LS} + D_{OL}$. $\Delta\alpha_n = \alpha - 2n\pi$ is the offset of the deflection angle, and n is an integer that indicates

the number of loops done by the photon around the black hole. Since the lensing effects are more significant when the objects are highly aligned, we will study the case which the angles β and θ are small. We can find that the angular separation between the lens and the n th relativistic image is

$$\theta_n \simeq \theta_n^0 + \frac{u_{ps}e_n(\beta - \theta_n^0)D_{OS}}{\bar{a}D_{LS}D_{OL}}, \quad (3.2)$$

with

$$\theta_n^0 = \frac{u_{ps}}{D_{OL}}(1 + e_n), \quad e_n = e^{\frac{\bar{b}-2n\pi}{\bar{a}}}, \quad (3.3)$$

where θ_n^0 is the image position corresponding to $\alpha = 2n\pi$. As $n \rightarrow \infty$, we can find that $e_n \rightarrow 0$ from Eq. (3.3), which implies that the minimum impact parameter u_{ps} and the asymptotic position of a set of images θ_∞ obey a simple form

$$u_{ps} = D_{OL}\theta_\infty. \quad (3.4)$$

Then, the magnification of the n th relativistic image is given by

$$\mu_n = \frac{1}{\frac{\beta}{\theta} \frac{\partial \beta}{\partial \theta}} \bigg|_{\theta_n^0} = \frac{u_{ps}^2 e_n (1 + e_n) D_{OS}}{\bar{a} \beta D_{OL}^2 D_{LS}}. \quad (3.5)$$

It is easy to find that the first relativistic image is the brightest, and the magnification decreases exponentially with n . Therefore, we only consider that the outermost and brightest image θ_1 is resolved as a single image, and all the remaining ones are packed together at θ_∞ [6, 20]. Thus, the angular image separation s between the first image and the packed others, and the ratio \mathcal{R} of the flux from the first image to those from all other images can be expressed as

$$s = \theta_1 - \theta_\infty = \theta_\infty e^{\frac{\bar{b}-2\pi}{\bar{a}}}, \quad \mathcal{R} = \frac{\mu_1}{\sum_{n=2}^{\infty} \mu_n} = e^{\frac{2\pi}{\bar{a}}}. \quad (3.6)$$

These two formulas can be easily inverted to get

$$\begin{aligned}\bar{a} &= \frac{2\pi}{\log \mathcal{R}}, \\ \bar{b} &= \bar{a} \log \left(\frac{\mathcal{R}s}{\theta_\infty} \right).\end{aligned}\tag{3.7}$$

For a given theoretical model, the strong deflection limit coefficients \bar{a} and \bar{b} and the minimum impact parameter u_{ps} can be obtained; then these three observables s , θ_∞ , and \mathcal{R} can be calculated. On the other hand, comparing them with astronomical observations, it will allow us to determine the nature of the black hole stored in the lensing.

To provide an example, let us consider the supermassive black hole in the Galactic center can be described by this solution. It has a mass $M = 4.4 \times 10^6 M_\odot$ [38], and it is situated at a distance from the Earth $D_{OL} = 8.5\text{kpc}$; so the ratio of the mass to the distance is $\frac{M}{D_{OL}} \approx 2.4734 \times 10^{-11}$. Hence, we can estimate the value of the coefficients and observables for gravitational lensing by combining with Eqs. (2.27), (3.4), and (3.6). We present the numerical value for the angular image position θ_∞ , the angular image separation s , and the relative magnitude r_m (which is related to \mathcal{R} by $r_m = 2.5 \log \mathcal{R}$) of the relativistic images in Figs. 5-7. We can find that the angular image position θ_∞ decreases with the increase of scalar hair S for either $\mu = 0$ case or $\omega = \frac{\pi}{2}$ case in Fig. 5. We also find that the θ_∞ grows with the increase of ω for fixed S and μ , and so does the change of θ_∞ with μ for fixed S and ω . Figures 3 and 5 show that the changes in θ_∞ and u_{ps} are the same, this is because θ_∞ and u_{ps} satisfy the geometrical relationship of $u_{ps} = D_{OL}\theta_\infty$. Furthermore, we get from Figs. 6 and 7 that the angular image separation s increases, while the relative magnitude r_m decreases with the increase of scalar hair S . It is interesting to find that for different ω and μ , each line of θ_∞ , s , and r_m intersects at $S \rightarrow 0$, which returns to the results of the standard Schwarzschild case for $\theta_\infty = 26.5095\mu$ arc sec, $s = 0.0331\mu$ arc sec, and $r_m = 6.82$ [20]. There is another situation ($\omega = \frac{\pi}{2}$, $\mu \rightarrow 1$) that can return to the results of the Schwarzschild case, they are plotted with black lines in the graph on the right of Figs. 5-7.

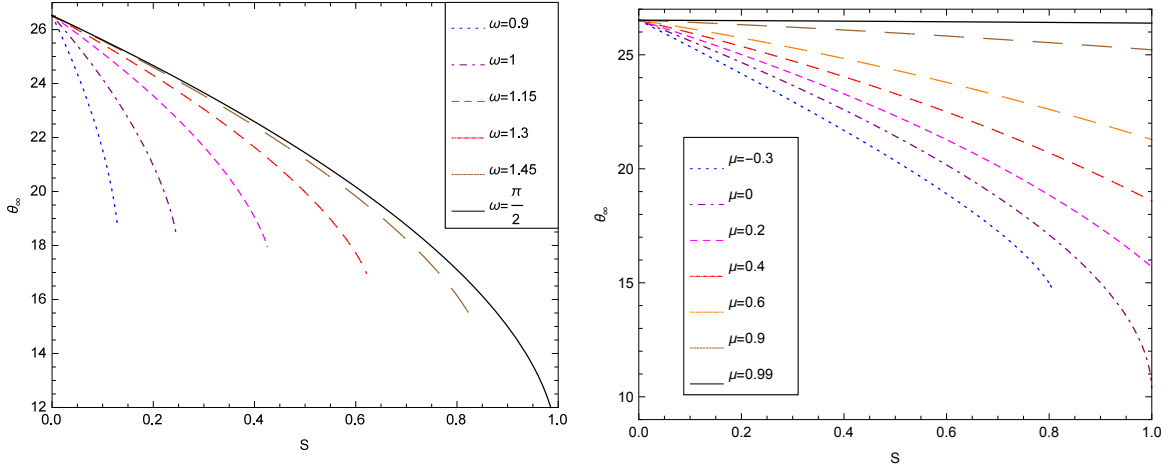


Figure 5: Gravitational lensing by the Galactic center black hole. Variation of the angular image position θ_∞ which is expressed in μ arc seconds with scalar hair S for $\mu = 0$ (left) and $\omega = \frac{\pi}{2}$ (right).

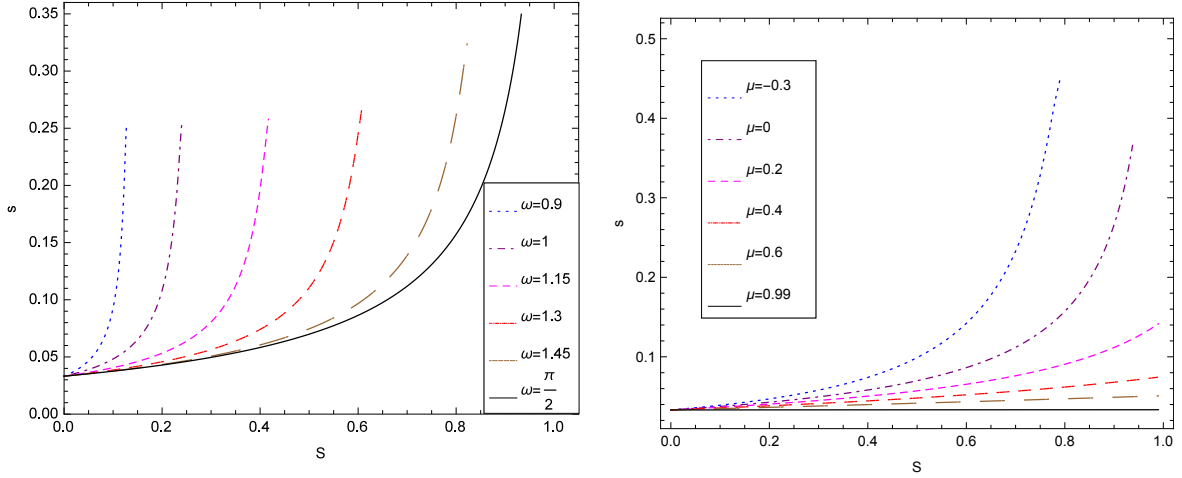


Figure 6: Gravitational lensing by the Galactic center black hole. Variation of the angular image separation s which is expressed in μ arc seconds with scalar hair S for $\mu = 0$ (left) and $\omega = \frac{\pi}{2}$ (right).

4. Time delay for charged black holes with scalar hair

Time delay is another observable for the bending of light rays, in addition to the angular image position θ_∞ , angular image separation s , and relative magnitude r_m . The above two sections are both studied in the photon sphere, and light goes around black hole for several times ($n \rightarrow \infty$). Then, the time delay is longer than the case that light does not loop

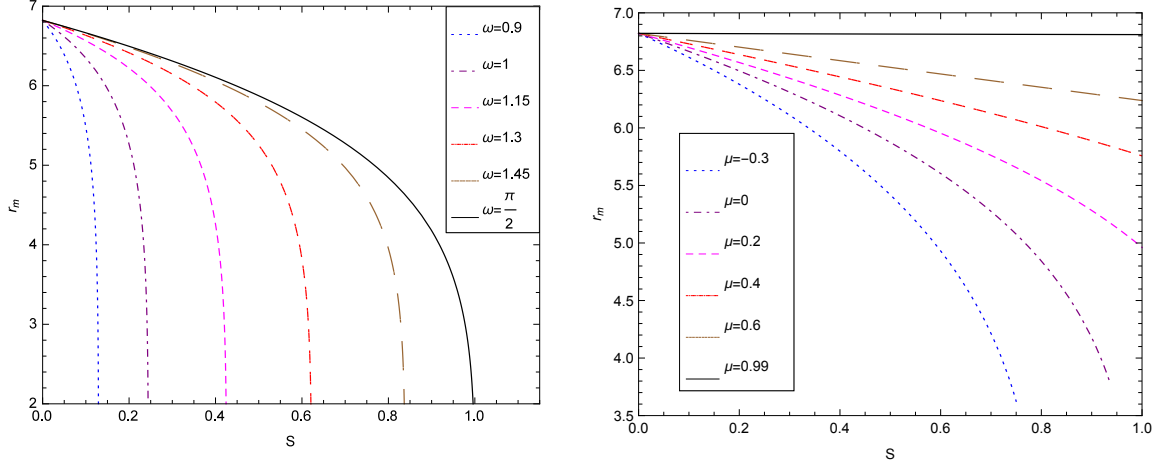


Figure 7: Gravitational lensing by the Galactic center black hole. Variation of the relative magnitude r_m with scalar hair S for $\mu = 0$ (left) and $\omega = \frac{\pi}{2}$ (right).

around the lens, and this is hard to observe. Therefore, in this part, we study the case that light does not loop around the lens ($n = 0$) and take the angular source position β as an independent variable which breaks the highly aligned hypothesis ($\beta \rightarrow 0$). Noting the fact that there are two relativistic images on each side of the object for fixed angular source position β , we mainly study the primary relativistic image which is on the same side of the source for simple.

Time delay of light traveling from the source to the observer with the closest distance of approach r_0 is defined as the difference between the light travel time for the actual ray in the gravitational field of the lens (deflector) and the travel time for the straight path between the source and the observer in the absence of the lens (i.e., if there is no gravitational field). From the null geodesics equation, Weinberg [39] got the time required for light to go from one point with $\{r, \theta = \frac{\pi}{2}, \varphi = \varphi_1\}$ to another point $\{r_0, \theta = \frac{\pi}{2}, \varphi = \varphi_2\}$ as

$$t(r, r_0) = t(r_0, r) = \int_{r_0}^r \sqrt{\frac{B(r)/A(r)}{1 - \frac{A(r)}{A(r_0)} \frac{C(r_0)}{C(r)}}} dr. \quad (4.1)$$

Then, the time delay of image by charged black holes with scalar hair can be expressed as [22, 23]

$$\tau(r_0) = 2M \left[\int_{r_0}^{\chi_s} \frac{dr}{F(r)} + \int_{r_0}^{\chi_o} \frac{dr}{F(r)} \right] - D_{OS} \sec\beta, \quad (4.2)$$

with

$$\begin{aligned} F(r) &= A(r) \sqrt{1 - \frac{A(r)}{A(r_0)} \frac{C(r_0)}{C(r)}}, \\ \chi_s &= \frac{D_{OS}}{2M} \sqrt{\left(\frac{D_{LS}}{D_{OS}} \right)^2 + \tan^2 \beta}, \\ \chi_o &= \frac{D_{OL}}{2M}, \end{aligned} \quad (4.3)$$

where, the first two terms in Eq. (4.2) stand for the travel time of the light from the source to the closest approach r_0 and from that point to the observer, and the last term denotes the travel time from the source to the observer in the absence of any gravitational field.

Now, we still use the same mass and distance as in the above part, but with an additional assumption which is $D_{OL} = D_{LS} = \frac{D_{OS}}{2}$, to estimate the time delay τ . From Table 1, we can find that, with the increase of the angular source position β , the time delay decreases remarkably, no matter how other variables change. This is because that the closest distance of approach r_0 increases with the increase of angular source position β , then the effect of the lens will be weakened, and its effect on the light will be reduced. We can also find that the time delay increases with the increase of scalar hair S for fixed ω and μ ; that is to say, the time delay for the charged black holes with scalar hair is always bigger than that of the Schwarzschild case. Furthermore, the time delay increases with the increase of ω and decreases with the increase of μ , but these variations are smaller than the variation causing by scalar hair S ; this shows that the scalar hair S has larger impact on the time delay than ω and μ .

5. Summary

In this paper we investigated gravitational lensing and time delay in the four dimensions charged black holes with scalar hair in the Einstein-Maxwell-Dilaton theory [37]. In Sec. 2, we studied the effects of the scalar hair on the strong deflection limit coefficient \bar{a} , the

(a) Time delay τ for $\mu = 0$ with the change of ω and scalar hair S .

β	$S = 0$	$\omega = 0.9$			$\omega = 1$			$\omega = 1.15$		
		$S = 0.2$	$S = 0.6$	$S = 1$	$S = 0.2$	$S = 0.6$	$S = 1$	$S = 0.2$	$S = 0.6$	$S = 1$
0	18.11567180	18.25992624	18.54843490	18.83694323	18.25992863	18.54844206	18.83695518	18.25992971	18.54844530	18.83696057
10^{-4}	18.11557239	18.25982684	18.54833549	18.83684383	18.25982923	18.54834266	18.83685577	18.25983031	18.54834590	18.83686117
10^{-2}	18.10574820	18.25000266	18.53851135	18.82701972	18.25000504	18.53851850	18.82703163	18.25000612	18.53852172	18.82703700
2	16.66483944	16.80909641	17.09761021	17.38612384	16.80909766	17.09761397	17.38613011	16.80909823	17.09761567	17.38613295
4	15.84711090	15.99136893	16.27988491	16.56840078	15.99136970	16.27988723	16.56840466	15.99137005	16.27988828	16.56840641

β	$S = 0$	$\omega = 1.3$			$\omega = 1.45$			$\omega = \frac{\pi}{2}$		
		$S = 0.2$	$S = 0.6$	$S = 1$	$S = 0.2$	$S = 0.6$	$S = 1$	$S = 0.2$	$S = 0.6$	$S = 1$
0	18.11567180	18.25993011	18.54844650	18.83696257	18.25993028	18.54844699	18.83696339	18.25993031	18.54844710	18.83696357
10^{-4}	18.11557239	18.25983071	18.54834709	18.83686316	18.25983087	18.54834759	18.83686398	18.25983091	18.54834769	18.83686416
10^{-2}	18.10574820	18.25000652	18.53852291	18.82703899	18.25000668	18.53852340	18.82703981	18.25000672	18.53852351	18.82703999
2	16.66483944	16.80909844	17.09761630	17.38613400	16.80909852	17.09761656	17.38613443	16.80909854	17.09761662	17.38613452
4	15.84711090	15.99137018	16.27988867	16.56840706	15.99137024	16.27988883	16.56840732	15.99137025	16.27988887	16.56840738

(b) Time delay τ for $\omega = \frac{\pi}{2}$ with the change of μ and scalar hair S .

β	$S = 0$	$\mu = -0.3$			$\mu = 0$			$\mu = 0.2$		
		$S = 0.5$	$S = 1$	$S = 2$	$S = 0.5$	$S = 1$	$S = 2$	$S = 0.5$	$S = 1$	$S = 2$
0	18.11567180	18.58451245	19.05335382	19.99103868	18.47631793	18.83696357	19.55825334	18.40418843	18.69270410	19.26973257
10^{-4}	18.11557239	18.58441305	19.05325441	19.99093928	18.47621853	18.83686416	19.55815393	18.40408902	18.69260469	19.26963316
10^{-2}	18.10574820	18.57458886	19.04343024	19.98111512	18.46639434	18.82703999	19.54832979	18.39426484	18.68278052	19.25980903
2	16.66483944	17.13368177	17.60252447	18.54021100	17.02548711	17.38613452	18.10742855	16.95335743	17.24187492	17.81890838
4	15.84711090	16.31595394	16.78479721	17.72248443	16.20775922	16.56840738	17.28970321	16.13562947	16.42414772	17.00118330

β	$S = 0$	$\mu = 0.4$			$\mu = 0.6$			$\mu = 0.99$		
		$S = 0.5$	$S = 1$	$S = 2$	$S = 0.5$	$S = 1$	$S = 2$	$S = 0.5$	$S = 1$	$S = 2$
0	18.11567180	18.33205906	18.54844518	18.98121403	18.25992983	18.40418683	18.69269772	18.11927824	18.12288465	18.13009734
10^{-4}	18.11557239	18.33195965	18.54834578	18.98111462	18.25983043	18.40408743	18.69259831	18.11917884	18.12278524	18.12999793
10^{-2}	18.10574820	18.32213547	18.53852160	18.97129048	18.25000624	18.39426325	18.68277416	18.10935464	18.11296105	18.12017374
2	16.66483944	16.88122782	17.09761561	17.53038939	16.80909829	16.95335659	17.24187157	16.66844591	16.67205236	16.67926519
4	15.84711090	16.06349976	16.27988825	16.71266411	15.99137009	16.13562895	16.42414565	15.85071738	15.85432384	15.86153674

Table 1: Numerical estimation for time delay τ for the black hole at the center of our Galaxy, which is supposed to be described by the charged black holes with scalar hair. Here, the angular source position β is expressed in *arc seconds*, and time delay τ is expressed in *minutes*.

minimum impact parameter u_{ps} , and the deflection angle $\alpha(\theta)$. We found from Figs. 2 and 4 that both the deflection angle $\alpha(\theta)$ and strong deflection limit coefficient \bar{a} increase with the increase of scalar hair for either $\mu = 0$ or $\omega = \frac{\pi}{2}$, which means that the deflection angle of light ray is dominated by the logarithmic term in gravitational lensing. Then, we showed that the minimum impact parameter u_{ps} decreases with the increase of scalar hair for either $\mu = 0$ or $\omega = \frac{\pi}{2}$. In Sec. 3, we studied the observables of gravitational lensing under the assumption that the observer, lens, and source are highly aligned. We learned from Figs. 3 and 5 that the changes of the angular image position θ_∞ and the minimum impact parameter u_{ps} are the same (both decrease with the increase of scalar hair) due to θ_∞ and u_{ps} satisfy the geometrical relationship of $u_{ps} = D_{OL}\theta_\infty$. Moreover, we also found, with the increase of scalar hair, that the angular image separation s increases, while the relative magnitude r_m decreases from Figs. 6 and 7. Then, in Sec. 4, we studied the time delay for the primary relativistic image, which is formed by the light does not

loop around the lens and situated on the same side of the source, and we took the angular source position β as an independent variable. We found that the time delay decreases with the increase of the angular source position remarkably, no matter how other variables change. This is because that the closest distance of approach r_0 increases with the increase of angular source position β , then the effect of the lens will be weakened, and its effect on the light will be reduced. We also found that the time delay increases with the increase of the scalar hair for every fixed ω and μ ; that is to say, the time delay for charged black holes with scalar hair is always bigger than that of the Schwarzschild case. It should be pointed out that this black hole can recover to the Schwarzschild black hole in two cases, one is $S \rightarrow 0$ for arbitrary ω and μ , another is $\omega = \frac{\pi}{2}$ and $\mu \rightarrow 1$ for arbitrary scalar hair, and all quantities of gravitational lensing can be reduced to those of the Schwarzschild spacetime— i.e., $r_H = 1$, $r_{ps} = 1.5$, $\bar{a} = 1$, $u_{ps} = 2.598$, $\alpha(\theta) = 6.28$, $\theta_\infty = 26.5095\mu$ arc sec, $s = 0.0331\mu$ arc sec, $r_m = 6.82$, $\tau = 18.11567180min$ ($\beta = 0$).

Acknowledgments

This work is supported by the National Natural Science Foundation of China under Grant Nos. 11475061; the Hunan Provincial Innovation Foundation for Postgraduate (Grant No.CX2016B164).

References

- [1] A. Einstein, *Lens-like action of a star by the deviation of light in the gravitational field*, Science **84**, 506 (1936).
- [2] F. W. Dyson, A. S. Eddington, and C. Davidson, *A determination of the deflection of light by the Sun's gravitational field, from observations made at the total eclipse of May 29, 1919*, Phil. Trans. Roy. Soc. Lond. A **220**, 291 (1920).
- [3] D. Walsh, R. F. Carswell, and R. J. Weymann, *0957 + 561 A, B: twin quasistellar objects or gravitational lens?* Nature **279**, 381 (1979).
- [4] K. S. Virbhadra and G. F. R. Ellis, *Schwarzschild black hole lensing*, Phys. Rev. D **62**, 084003 (2000).

- [5] S. Frittelly, T. P. Kling, and E. T. Newman, *Spacetime perspective of Schwarzschild lensing*, Phys. Rev. D **61**, 064021 (2000).
- [6] V. Bozza, *Quasiequatorial gravitational lensing by spinning black holes in the strong field limit*, Phys. Rev. D **67**, 103006(2003).
- [7] E. F. Eiroa, *Braneworld black hole gravitational lens: Strong field limit analysis*, Phys. Rev. D **71**, 083010 (2005); E. F. Eiroa, *Gravitational lensing by Einstein-Born-Infeld black holes*, Phys. Rev. D **73**, 043002 (2006); E. F. Eiroa and C. M. Sendra, *Regular phantom black hole gravitational lensing*, Phys. Rev. D **88**, 103007 (2013).
- [8] R. Whisker, *Strong gravitational lensing by braneworld black holes*, Phys. Rev. D **71**, 064004 (2005).
- [9] G. N. Gyulchev and S. S. Yazadjiev, *Kerr-Sen dilaton-axion black hole lensing in the strong deflection limit*, Phys. Rev. D **75**, 023006 (2007); G. N. Gyulchev and S. S. Yazadjiev, *Gravitational lensing by rotating naked singularities*, Phys. Rev. D **78**, 083004 (2008).
- [10] A. Bhadra, *Gravitational lensing by a charged black hole of string theory*, Phys. Rev. D **67**, 103009 (2003).
- [11] T. Ghosh and S. Sengupta, *Strong gravitational lensing across a dilaton anti-de Sitter black hole*, Phys. Rev. D **81**, 044013 (2010).
- [12] A. N. Aliev and P. Talazan, *Gravitational effects of rotating braneworld black holes*, Phys. Rev. D **80**, 044023 (2009).
- [13] C. Ding, C. Liu, Y. Xiao, L. Jiang, and R. Cai, *Strong gravitational lensing in a black-hole spacetime dominated by dark energy*, Phys. Rev. D **88**, 104007 (2013); S. Wei, Y. Liu, C. Fu, and K. Yang, *Strong field limit analysis of gravitational lensing in Kerr-Taub-NUT spacetime*, JCAP **10**, 053 (2012); S. Wei and Y. Liu, *Equatorial and quasiequatorial gravitational lensing by a Kerr black hole pierced by a cosmic string*, Phys. Rev. D **85**, 064044 (2012).
- [14] G. V. Kraniotis, *Precise analytic treatment of Kerr and Kerr-(anti) de Sitter black holes as gravitational lenses*, Class. Quant. Grav. **28**, 085021 (2011).

- [15] J. Sadeghi, J. Naji, and H. Vaez, *Strong gravitational lensing in a charged squashed Kaluza-Klein Gödel black hole*, Phys. Lett. B **728**, 170 (2014); J. Sadeghi, A. Banijamali, and H. Vaez, *Strong gravitational lensing in a charged squashed Kaluza-Klein black hole*, Astrophys Space Sci. **343**, 559 (2013).
- [16] V. Bozza, F. De Luca, G. Scarpetta, and M. Sereno, *Analytic Kerr black hole lensing for equatorial observers in the strong deflection limit*, Phys. Rev. D **72**, 083003 (2005); V. Bozza, F. De Luca, and G. Scarpetta, *Kerr black hole lensing for generic observers in the strong deflection limit*, Phys. Rev. D **74**, 063001 (2006).
- [17] C. Darwin, *The gravity field of a particle*, Proc. Roy. Soc. Lond. A **249**, 180 (1959).
- [18] J. P. Luminet, *Image of a spherical black hole with thin accretion disk*, Astron. Astrophys. **75**, 228 (1979); H. C. Ohanian, *The black hole as a gravitational “lens”*, Am. J. Phys. **55**, 428 (1987); R. J. Nemiroff, *Visual distortions near a neutron star and black hole*, Am. J. Phys. **61**, 619 (1993); V. Bozza, S. Capozziello, G. Iovane, and G. Scarpetta, *Strong field limit of black hole gravitational lensing*, Gen. Rel. and Grav. **33**, 1535 (2001).
- [19] E. F. Eiroa, G. E. Romero, and D. F. Torres, *Reissner-Nordström black hole lensing*, Phys. Rev. D **66**, 024010 (2002).
- [20] V. Bozza, *Gravitational lensing in the strong field limit*, Phys. Rev. D **66**, 103001 (2002).
- [21] S. Chen and J. Jing, *Strong field gravitational lensing in the deformed Hořava-Lifshitz black hole*, Phys. Rev. D **80**, 024036 (2009); Y. Liu, S. Chen, and J. Jing, *Strong gravitational lensing in a squashed Kaluza-Klein black hole spacetime*, Phys. Rev. D **81**, 124017 (2010); S. Chen and J. Jing, *Geodetic precession and strong gravitational lensing in dynamical Chern-Simons-modified gravity*, Class. Quant Grav. **27**, 225006, (2010); S. Chen, Y. Liu, and J. Jing, *Strong gravitational lensing in a squashed Kaluza-Klein Gödel black hole*, Phys. Rev. D **83**, 124019 (2011); C. Ding, S. Kang, C. Chen, S. Chen, and J. Jing, *Strong gravitational lensing in a noncommutative black-hole spacetime*, Phys. Rev. D **83**, 084005, (2011); S. Chen and J. Jing, *Strong gravitational lensing by a rotating non-Kerr compact object*, Phys. Rev. D **85**, 124029 (2012); C. Liu, S. Chen, and J. Jing, *Strong gravitational lensing of quasi-Kerr compact object with arbitrary quadrupole moments*, J. High Energy Phys. **08**, 097 (2012); L. Ji, S. Chen, and J. Jing, *Strong gravitational lensing in a rotating*

- Kaluza-Klein black hole with squashed horizons*, J. High Energy Phys. **03**, 089 (2014); S. Chen and J. Jing, *Strong gravitational lensing for the photons coupled to Weyl tensor in a Schwarzschild black hole spacetime*, JCAP **10**, 002 (2015).
- [22] K. S. Virbhadra and C. R. Keeton, *Time delay and magnification centroid due to gravitational lensing by black holes and naked singularities*, Phys. Rev. D **77** 124014 (2008).
- [23] K. S. Virbhadra, *Relativistic images of Schwarzschild black hole lensing*, Phys. Rev. D **79** 083004 (2009).
- [24] R. Ruffini and J. A. Wheeler, *Introducing the black hole*, Physics Today **24**, 30 (1971).
- [25] M. Nadalini, L. Vanzo, and S. Zerbini, *Thermodynamical properties of hairy black holes in n spacetime dimensions*, Phys. Rev. D **77**, 024047 (2008).
- [26] A. Anabalon, *Exact black holes and universality in the backreaction of non-linear sigma models with a potential in $(A)dS_4$* , J. High Energy Phys. **06**, 127 (2012).
- [27] C. A. R. Herdeiro and E. Radu, *Kerr black holes with scalar hair*, Phys. Rev. Lett. **112**, 221101 (2014).
- [28] C. Martinez and J. Zanelli, *Conformally dressed black hole in $2 + 1$ dimensions*, Phys. Rev. D **54**, 3830 (1996).
- [29] G. Aad et al, *Observation of a new particle in the search for the Standard Model Higgs boson with the ATLAS detector at the LHC*, Phys. Lett. B **716**, 1 (2012).
- [30] S. Chatrchyan et al, *Observation of a new boson at a mass of 125 GeV with the CMS experiment at the LHC*, Phys. Lett. B **716**, 30 (2012).
- [31] A. Sagnotti, *A note on the Green-Schwarz mechanism in open-string theories*, Phys. Lett. B **294**, 196 (1992).
- [32] M. J. Duff and J. X. Lu, *Loop expansions and string/five-brane duality*, Nucl. Phys. B **357**, 534 (1991).
- [33] J. Erler, *Anomaly cancellation in six dimensions*, J. Math. Phys. **35**, 1819 (1994).
- [34] F. Faedo, D. Klemm, and M. Nozawa, *Hairy black holes in $N = 2$ gauged supergravity*, arXiv:1505.02986.

- [35] G. Dall'Agata, G. Inverso, and M. Trigiante, *Evidence for a family of $SO(8)$ gauged supergravity theories*, Phys. Rev. Lett. **109**, 201301 (2012).
- [36] G. W. Gibbons and K. i. Maeda, *Black holes and membranes in higher-dimensional theories with dilaton fields*, Nucl. Phys. B **298**, 741 (1988).
- [37] Z. Y. Fan and H. Lu, *Charged black holes with scalar hair*, J. High Energy Phys. **09**, 060 (2015).
- [38] R. Genzel, F. Eisenhauer, and S. Gillessen, *The Galactic Center massive black hole and nuclear star cluste*, Rev. Mod. Phys. **82**, 3121 (2010).
- [39] S. Weinberg, *Gravitation and Cosmology: principles and applications of the general theory of relativity* (Wiley, New York, 1972).